Perspective of Quantum Decoherence from Holography and Majorana Modes

Feng-Li Lin(NTNU &NCTS)

Based on

1. arXiv:1309.5855(JHEP 1401 (2014) 170) with Shih-Hao Ho(NCTS), Wei-Li(AEI->ITP) and Bo Ning(NTNU->SCU).

2. arXiv:1406.6249(NJP 16 (2014) 113062) with Shi-Hao Ho(NCTS), Sung-Po Chao(NCTS->ASIOP) & Chung-Hsien Chou(NCKU)

3. on-going work with Pei-Hua Liu(NTNU) and Jen-Tsung Hsiang(Fudan U)

Motivation

1. Study the quantum decoherence of strongly coupled/correlated systems. E.g. Luttinger liquid.

2. Bring attention to the relation between Schwinger-Keldysh and Feynman-Vernon formalisms.

3. Identify the ingredients for making the robust (topological) qubits against decoherence.

4. A novel way to tackle the decoherence of fermionic qubits.

Feynman-Vernon formalism

- Using

$$\langle \bar{\phi}_+, \bar{\chi}_+ | e^{-iH(t_f - t_i)} | \tilde{\phi}_+, \tilde{\chi}_+ \rangle = \int_{\tilde{\phi}_+}^{\bar{\phi}_+} \mathcal{D}\phi_+ \int_{\tilde{\chi}_+}^{\bar{\chi}_+} \mathcal{D}\chi_+ \; e^{i \int_{t_i}^{t_f} dt \; \mathcal{L}[\phi_+, \chi_+]}$$

$$\langle \tilde{\phi}_-, \tilde{\chi}_- | e^{iH(t_f - t_i)} | \bar{\phi}_-, \bar{\chi}_- \rangle = \int_{\tilde{\phi}_-}^{\bar{\phi}_-} \mathcal{D}\phi_- \int_{\tilde{\chi}_-}^{\bar{\chi}_-} \mathcal{D}\chi_- \; e^{-i \int_{t_i}^{t_f} dt \; \mathcal{L}[\phi_-, \chi_-]}$$

- Then we have influence functional

$$\mathcal{F}[\phi_+, \phi_-] \equiv \int d\bar{\chi} \, d\tilde{\chi}_+ \, d\tilde{\chi}_- \, \langle \tilde{\chi}_+ | \hat{\rho}_{\rm env}(t_i) | \tilde{\chi}_- \rangle \cdot \int_{\tilde{\chi}_+}^{\bar{\chi}} \mathcal{D}\chi_+ \int_{\tilde{\chi}_-}^{\bar{\chi}} \mathcal{D}\chi_- e^{-i \int_{t_i}^{t_f} dt (\mathcal{L}_{\rm env}[\chi_+] - \mathcal{L}_{\rm env}[\chi_-] + \mathcal{L}_{\rm int}[\phi_+, \chi_+] - \mathcal{L}_{\rm int}[\phi_-, \chi_-])}$$

- RDM:

$$\langle \bar{\phi}_+ | \hat{\rho}_{\rm sys}(t_f) | \bar{\phi}_- \rangle = \int d\tilde{\phi}_+ d\tilde{\phi}_- J \left[\bar{\phi}_+, \bar{\phi}_-; t_f | \tilde{\phi}_+, \tilde{\phi}_-; t_i \right] \langle \tilde{\phi}_+ | \hat{\rho}_{\rm sys}(t_i) | \tilde{\phi}_- \rangle$$

- RDM propagator:

$$J \left[\bar{\phi}_+, \bar{\phi}_-; t_f | \tilde{\phi}_+, \tilde{\phi}_-; t_i \right] \equiv \int_{\tilde{\phi}_+}^{\bar{\phi}_+} \mathcal{D}\phi_+ \int_{\tilde{\phi}_-}^{\bar{\phi}_-} \mathcal{D}\phi_- \; e^{i \int_{t_i}^{t_f} dt \; (\mathcal{L}_{\rm sys}[\phi_+] - \mathcal{L}_{\rm sys}[\phi_-])} \mathcal{F}[\phi_+, \phi_-]$$

FV vs Schwinger-Keldysh

cf. Su, Chen, Yu, Zhou

- The FV influence functional can be compactly written as:

$$\mathcal{F}[\phi_+,\phi_-] = \left\langle e^{ig\int_C d^{d+1}x\ \phi\ \mathcal{O}[\chi]} \right\rangle_\chi \quad \text{for} \quad \mathcal{L}_{int}[\phi,\chi] = g\ \phi\ \mathcal{O}[\chi]$$

- This can be understood as the **generating functional for the real-time correlations of** $\mathcal{O}[\chi]$ **in SK formalism**.
- Here the **probe acts as the external source** to $\mathcal{O}[\chi]$.
- The probe loses its **purity** via a particular **channel** $\mathcal{O}[\chi]$.
- Using **Kubo formula**, one can then relate the transport coefficient to the retarded Green function in the context of linear response theory.

$$\chi^O = -\lim_{\omega\to 0}\lim_{\vec{k}\to 0}\frac{1}{\omega}\mathrm{Im}\,G_R^O(\omega,\vec{k})$$

SK formalism

- For Gaussian environment:

$$-i\ln\mathcal{F}[\phi_+,\phi_-] = -\frac{g^2}{2}\int d^{d+1}x \int d^{d+1}x' \sum_{s,s'} \mathrm{sgn}(ss')\phi^s(x)G_{ss'}(x-x')\phi^{s'}(x')$$

$$G_{ss'}(1,2)| \equiv -i\langle \mathcal{T}_{\mathcal{K}}\mathcal{O}_s(1)\mathcal{O}_{s'}(2)\rangle_{\mathrm{env}}$$

- By the causality principle, only 3 of the $G_{ss'}$ are independent. Perfoming Keldysh rotation so that only G_R & G_{sym} appear in the influence functional:

$$\Sigma = \frac{1}{2}(\phi_+ + \phi_-)\,, \qquad \Delta = \phi_+ - \phi_-$$

$$-i\ln\mathcal{F} = -g^2\int_{t_i}^{t_f} d\tau \int_{t_i}^{t_f} d\tau' \int d^dx\, d^dx' \,[\Delta(x)G_R(x-x')\Sigma(x') - \frac{i}{2}\Delta(x)G_{sym}(x-x')\Delta(x')]$$

$$G_R(t,t') = \theta(t-t')[G_{-+}(t,t') - G_{+-}(t,t')] \qquad G_{sym}(t,t') = G_{-+}(t,t') - G_{+-}(t,t')$$

I. Holographic Quantum Decoherence

Holographic Influence Functional

c.f. Maldacena, 1997; Gubser, Klebanov & Polyakov, 1998; Witten 1998; Maldacena, 2003; Son & Herzog, 2003

- Influence functional = Generating function of real-time correlation function.
- AdS/CFT duality: Effective theory for a strongly coupled CFT is a co-dimensional 1 higher AdS gravity. Precisely,

- Still $$\mathcal{F}^{(h)}[\phi] := \left\langle e^{ig\int_C d^{d+1}x\,\phi\,\mathcal{O}[\chi]} \right\rangle_\chi = e^{iS_{bulk}[\Phi|_\phi]}$$

$$-i\ln\mathcal{F} = -g^2\int_{t_i}^{t_f} d\tau \int_{t_i}^{t_f} d\tau' \int d^dx\, d^dx'\, [\Delta(x)G_R(x-x')\Sigma(x') - \frac{i}{2}\Delta(x)G_{sym}(x-x')\Delta(x')]$$

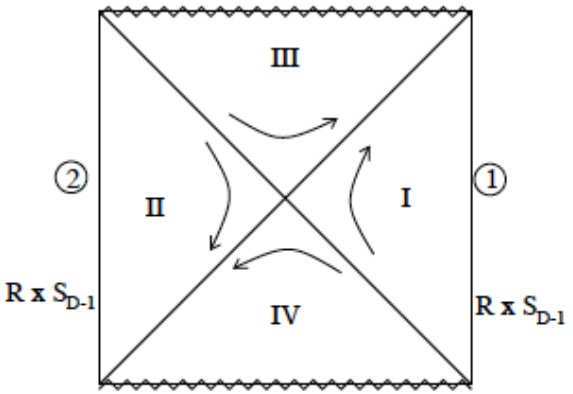

Holographic Green function

- GKP/W prescription:

$$\exp\left(-S_{bulk}^{(on-shell)}[\phi]\right) = \left\langle \exp\int \phi_{nn}^{(b)} O \right\rangle_{CFT}$$

- Solve bulk EOMs:

$$\phi(t,\vec{x},z) \sim \phi_{nn}^{(b)}(t,\vec{x}) z^{\Delta_{nn}} + \phi_{n}^{(b)}(t,\vec{x}) z^{\Delta_{n}}, \Delta_n > \Delta_{nn}.$$

source $J(t,\vec{x})$ response $\langle O(t,\vec{x})\rangle$

For black hole, one needs to impose incoming b.c. to obtain retarded Green function.

- Linear response theory:

$$\left\langle O(\omega,\vec{k})\right\rangle = -G_R^O(\omega,\vec{k}) J(\omega,\vec{k})$$

$$\chi^O = -\lim_{\omega\to 0}\lim_{\vec{k}\to 0}\frac{1}{\omega}\mathrm{Im}\, G_R^O(\omega,\vec{k})$$

Holographic Environmental Kernels

c.f. Son & Teaney, 2009; de Boer, Rangamani & Shigemori, 2009

1. The thermal kicks of the Hawking radiation causes Brownian motion of the end-point.

The dissipation kernel for this holographic Brownian motion is super-Ohmic like:

$$G_R(\omega) = -iN_{st}^2\left(\omega^3 + 4\pi^2T^2\omega\right)\frac{\Gamma_w^2}{\Gamma_w^2+\omega^2}$$

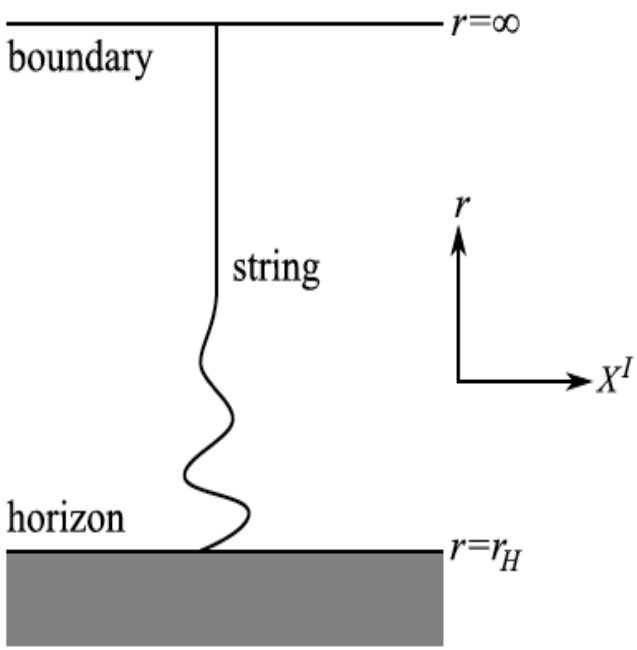

2. C.f. the dissipation kernel for k=0 scalar mode in AdS5 is quasi-super-Ohmic:

$$G_R(\omega) \propto (\omega^2)^{2\Delta-2}[\ln\omega^2 - i\pi\mathrm{sgn}(\omega)] \qquad \text{for} \quad \Delta \geq 2$$

Environmental Kernels

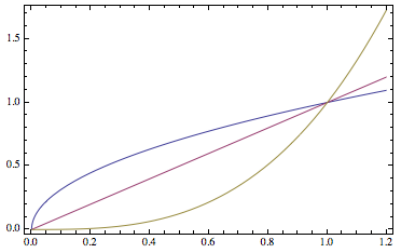

- The above environmental kernels are of the Ohmic type spectra:

$$S_{spec}^{(env)}(\omega) = c_0(Q)\omega^Q \, e^{-\omega^2/\Gamma_0^2} \, , \qquad Q \geq 0$$

- This is the typical spectra for the helical Luttinger liquid: Q=1 (Ohmic, Fermi-liquid), Q<1 (sub-Ohmic, attarctive interaction), Q>1 (super-Ohmic, repulsive interaction).

- Non-Ohmic environmental kernel, such as the free spectra or the holographic ones, i.e., the holographic strange metal:

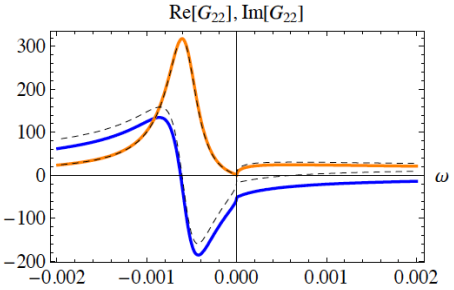

k<kF

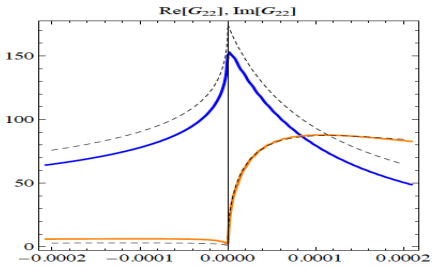

k>kF

Holographic decoherence behaviors

Characterize Decoherence (for continuous variables)

- Positivity of Wigner function (quantum version of phase space probability distribution function):

$$W(\bar{\Sigma}, p, t) := \frac{1}{2\pi} \int_{-\infty}^{\infty} d\bar{\Delta}\, \rho_{sys}(\bar{\Sigma} + \frac{\bar{\Delta}}{2}, \bar{\Sigma} - \frac{\bar{\Delta}}{2}, t)\, e^{-ip\bar{\Delta}}.$$

- For 2 Gaussian wave-packets (qubit of continuous variables):

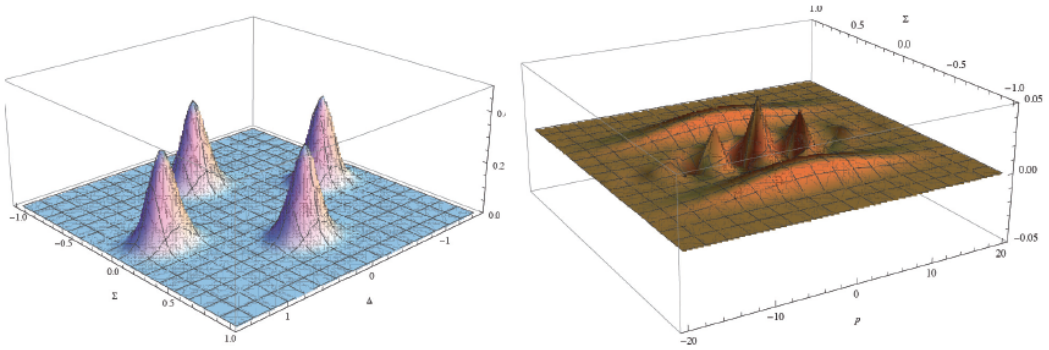

FIG. 3. Left: Density matrix and Right: Wigner function of two Gaussian wave-packets given by

Evolve Wigner function

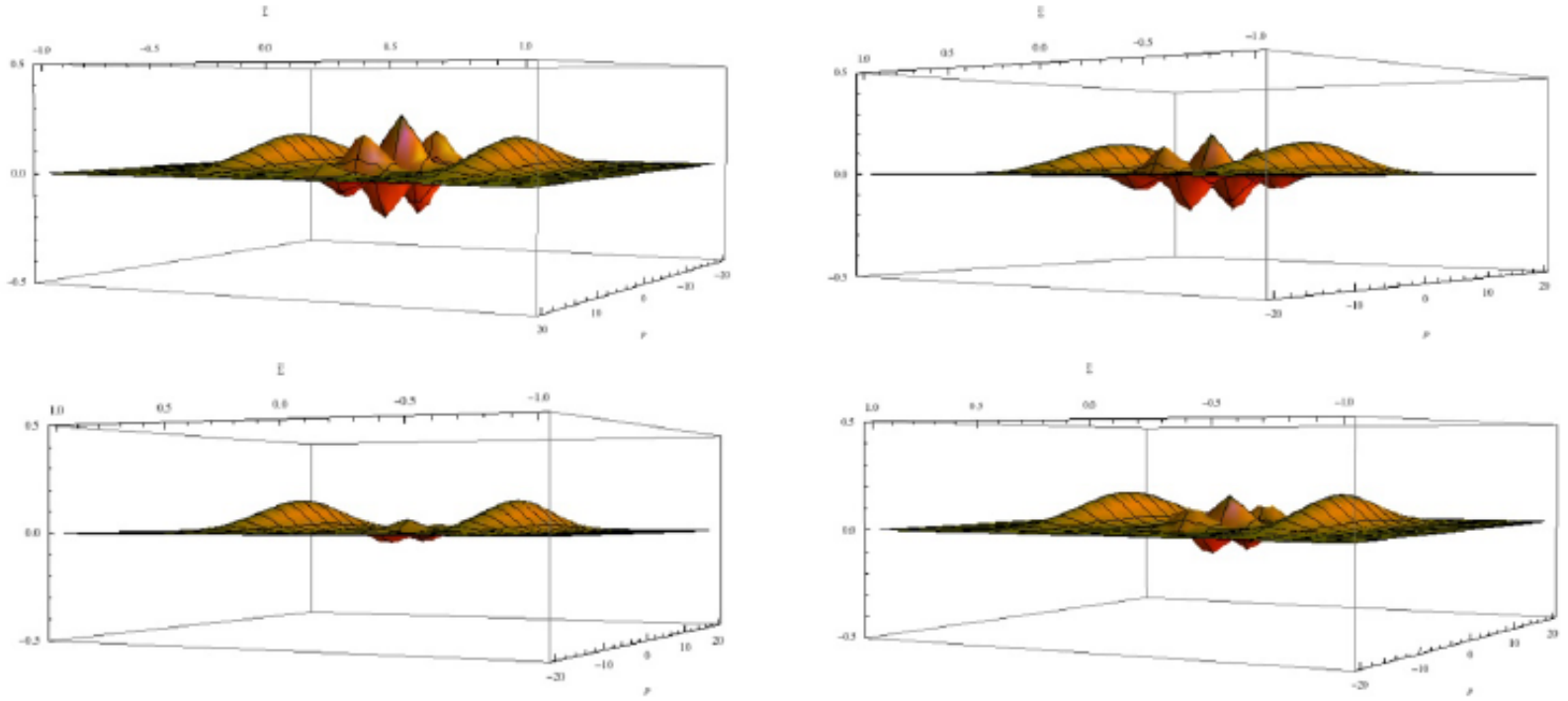

Figure 5. The evolution of the Wigner function $W(\Sigma, p, t)$ for the two Gaussian wave-packets made of the scalar ϕ with $\Delta_{\mathcal{O}} = 3$. The evolution goes clockwise as $t = 10$, $t = 15$, $t = 20$ and $t = 30$ units respectively.

Purity and Concurrence

- If the state of the qubits does not reduce to a pointer state, it means the decoherence is incomplete, and could be further purified. Then we can characterize the purity by

$$\mathcal{P} := Tr\rho_r^2(t)$$

- For two-qubit state, we can characterize the quantum entanglement between the two qubits by concurrence:

$$\mathcal{C}(\rho_r) := max(0, \lambda_1 - \lambda_2 - \lambda_3 - \lambda_4)$$

$\lambda_1, \lambda_2, \lambda_3, \lambda_4$ are the square roots of eigenvalues, in decreasing order, of $\rho_r(\sigma_y \otimes \sigma_x)\rho_r^*(\sigma_y \otimes \sigma_x)$.

- Zero concurrence implies no entanglement, but the state could be still quantum.

Generic Behaviors for W & S2

- Case 1. T=50(red), 30(green) and 0.1(blue)

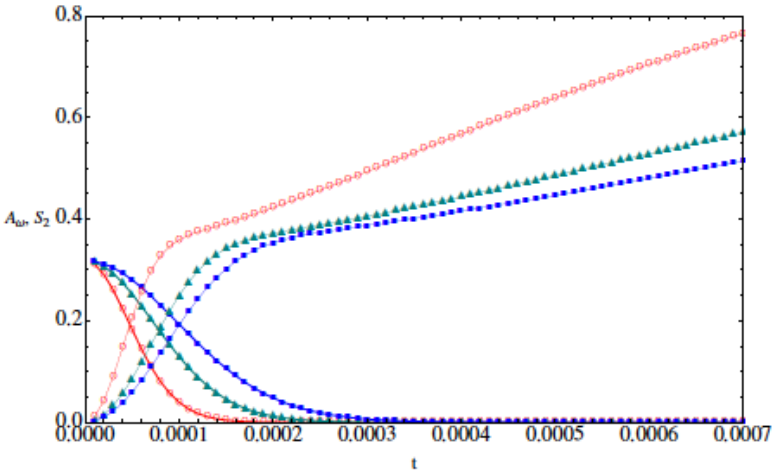

- Case 2. Delta=4.5(green), 4(red) and 3.5(blue)

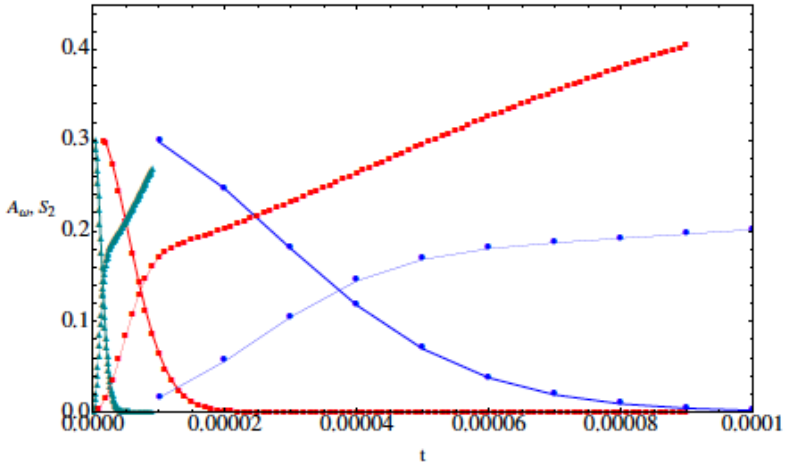

Decoherence v.s. Local Quench

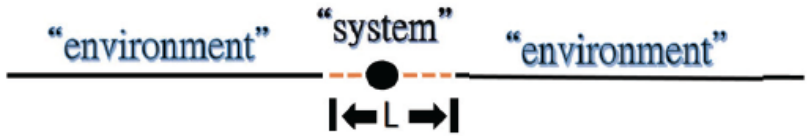

- Local quantum quench: A local excitation is created suddenly and see how it relaxes back the equilibrium.
- The thermalization is characterized by a Gibbs state RDM.

- If the local excitation is a quantum state, then its purity will escape into the rest of the total system. This is the quantum decoherence.
- The decoherence is characterized by a pointer state RDM.

Decoherence v.s. local quench

- Local quantum quench (CFT + holographic calculations):

c.f. Liu & Suh, 2014

$$S_L(t) \sim \begin{cases} t^2, & t \approx 0\,; \\ t, & t < L\,; \\ \text{const. or} \quad \ln t, & t > L\,. \end{cases}$$

- Quantum decoherence (Our fittings):

$$S_2(t) \sim \begin{cases} C_0\, t^2\,, & t \approx 0\,; \\ C_{b.c.}\, t\,, & t < t_D\,; \\ C_{a.c.} \ln t\,, & \mathcal{O}(10)\, t_D > t > t_D\,; \\ C_1\, t\,, & t >> t_D\,. \end{cases}$$

$$C_{b.c.} > C_1$$

Scaling behaviors

- For Case 1, we find the decoherence time t_D is independent of temperature T at low T regime, and at high T regime, it behaves as

$$t_D \sim \frac{1}{T}.$$

- As in CFT, there is only a time scale set by 1/T, which is approximately the thermalization time scale. However, the time for the complete thermalization for a continuous variable probe takes infinitely long.

- For Case 2, we consider T=0 case but with different conformal dimension Delta of operator O[x], we find

$$\ln t_D \sim - C_\Delta \Delta_\mathcal{O}$$

II. Decoherence of Fermionic Qubits

The generalized quadratic fermion model

- The model Hamiltonian is for a (few) spinless fermionic qubit(s) interacting with the fermonic bath:

$$H = H_p + H_E + V$$

$$a|1\rangle = |0\rangle$$
$$a^\dagger|0\rangle = |1\rangle$$

$$V = aO^\dagger + Oa^\dagger, \qquad \{a, a^\dagger\} = 1$$

$$O = \sum_\omega [C(\omega)b_\omega + D(\omega)b_\omega^\dagger]$$

- Formally we can decompose the spinless fermions in to pairs of Majorana modes, and the Hamiltonian becomes

$$V = \gamma_1 O_1 + \gamma_2 O_2$$

$$\gamma_1 = a + a^\dagger, \qquad \gamma_2 = i(a^\dagger - a)$$

$$O_1 = (O - O^\dagger)/2, \qquad O_2 = (O + O^\dagger)/2i$$

$$\gamma_a^\dagger = \gamma_a, \ \{\gamma_a, \gamma_b\} = 2\delta_{ab}$$

Issues about decoherence of fermionic qubits

- To adopt the path-integral Fenyman-Vernon method, we need to choose the coherent state basis with fermionic Grassmann eigenvalues.

- This was done in WM Zhang et al (2012, PRL) for the environment with Lorentzian spectra density.

- However, we found that the formalism fails to produce a positive-definite RDM for large probe kinetic energy.

- We try to use alternative way to evaluate RDM.

Purity for RDM of a Dirac fermion probe in fermionic bath

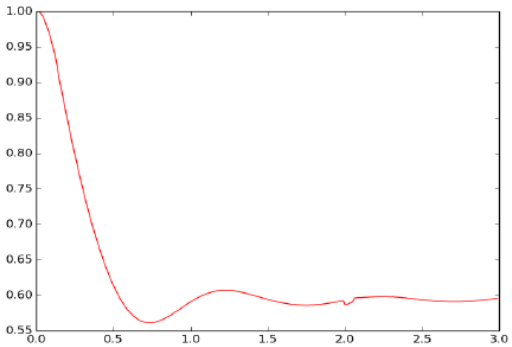

FIG. 5: $Tr\rho^2$ for Lorentz spectral density case with E=5.0 and initial state $\frac{1}{\sqrt{2}}|0\rangle + \frac{1}{\sqrt{2}}|1\rangle$.

in Fig.6, we find $Tr\rho^2$ may be larger than 1.

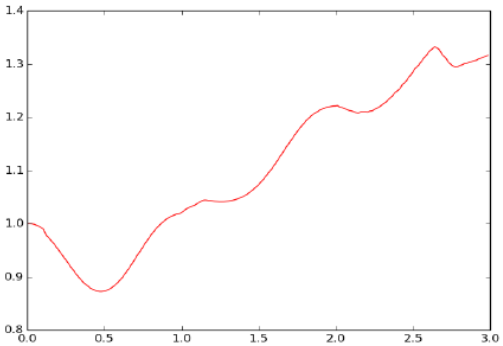

FIG. 6: $Tr\rho^2$ for Super-Ohmic case with $\kappa = 3/2$, E=5.0 and initial state $\frac{1}{\sqrt{2}}|0\rangle + \frac{1}{\sqrt{2}}|1\rangle$.

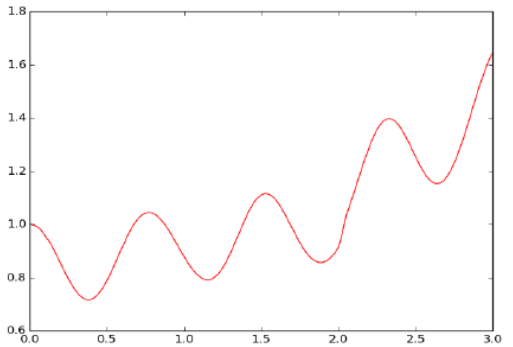

FIG. 7: $Tr\rho^2$ for Sub-Ohmic case with $\kappa = 3/5$, E=5.0 and initial state $\frac{1}{\sqrt{2}}|0\rangle + \frac{1}{\sqrt{2}}|1\rangle$.

4. Lorentz spectral density case (E=100): as showed in Fig.8, we find if E is very large , even for Lorentz spectral density case , $Tr\rho^2$ may be larger than 1.

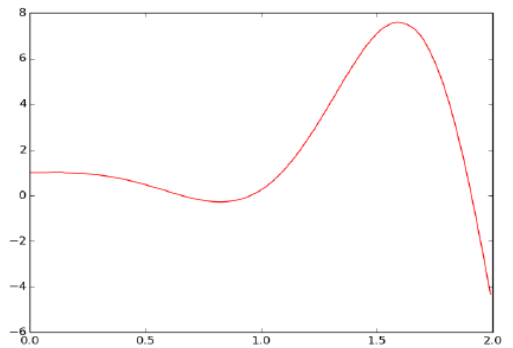

FIG. 8: $Tr\rho^2$ for Lorentz spectral density case with E=100.0 and initial state $\frac{1}{\sqrt{2}}|0\rangle + \frac{1}{\sqrt{2}}|1\rangle$.

Canonical formulation of RDM

- Instead of using Feynman-Vernon, we now use canonical formulation in the interaction picture. Then, the RDM takes the form:

$$\rho_r(t) = e^{-iH_p t}(Tr_E U(t)\rho_0 U^\dagger(t))e^{iH_p t}$$

$$\rho_0 = \rho_p \otimes \rho_E, \qquad U(t) = Te^{-i\int^t d\tau V_I(\tau)}$$

$$V_I(t) = e^{i(H_p+H_E)t}(aO^\dagger + Oa^\dagger)e^{-i(H_p+H_E)t}$$

- Even this is just a quadratic model, it is quite difficult to evaluate RDM in a closed form due to the complication of mixed normal ordering for ``a" and ``O" operators.

Dressing by the Majorana mode

- In terms of Majorana basis, we have

$$V_I(t) = \gamma_1(t)O_1(t) + \gamma_2(t)O_2(t)$$

so that the evolution operator is in the form

$$U(t) = Te^{\gamma_a Q_a(t)}, \qquad Q_a(t) = i\int_t d\tau \mathcal{Q}_a(\tau)$$

Key Observation: **Under time ordering** and due to the dressing by Majorana modes, Q_a can be thought as **the bosonic and mutually fermionic**.

$$T\gamma_1 Q_1(t)\gamma_1 Q_1(t) = -\int^t \int^t [\theta(\tau-\tau')\mathcal{Q}_1(\tau)\mathcal{Q}_1(\tau') + (\tau \leftrightarrow \tau')]$$

$$T\gamma_1 Q_1(t)\gamma_2 Q_2(t) = T\gamma_2 Q_2(t)\gamma_1 Q_1(t)$$
$$= -\gamma_1\gamma_2 \int^t \int^t [\theta(\tau-\tau')\mathcal{Q}_1(\tau)\mathcal{Q}_2(\tau') - \theta(\tau'-\tau)Q_2(\tau')Q_!(\tau)]$$

RDM in closed form

- By the above observation, we can eliminate gamma's by Clifford algebra without worrying about the mixed normal ordering.

- In the mean-time, just treat Q_a as the commuting operators as the bosonic/fermionic feature is implicitly hidden in the time ordering.

- In the end of the day, the RDM has the following form:

$$\rho_r(t) = {}_E\langle 0|U_\nu^\dagger(t)U_\mu(t)|0\rangle_E \Gamma_\mu \rho_P \Gamma_\nu^\dagger$$
$$\Gamma_0 = 1,\ \Gamma_1 = \gamma_1,\ \Gamma_2 = \gamma_2,\ \Gamma_3 = -\gamma_1\gamma_2,$$
$$U_0(t) = T\cos O_1 \cos O_2,\ U_1(t) = T\sin O_1 \cos O_2$$
$$U_2(t) = T\cos O_1 \sin O_2,\ U_3(t) = T\sin O_1 \sin O_2$$

Assume O_a are generalized free fields:

$$
\begin{aligned}
&U_0(t) = T\cos O_1 \cos O_2 \\
&= T\frac{e^{iO_1}+e^{-iO_1}}{2}\frac{e^{iO_2}+e^{-iO_2}}{2} \\
&= \frac{1}{4}T\left[e^{i(O_1+O_2)}+e^{-i(O_1+O_2)}+e^{i(O_1-O_2)}+e^{-i(O_1-O_2)}\right] \\
&= \frac{1}{4}e^{\left[\frac{1}{2}\int^t\int^t\langle TO(\tau)O(\tau')\rangle d\tau d\tau'\frac{\delta}{\delta O(\tau)}\frac{\delta}{\delta O(\tau')}\right]}\left\{:e^{i(O_1+O_2)}:+:e^{-i(O_1+O_2)}:+:e^{i(O_1-O_2)}:+:e^{-i(O_1-O_2)}:\right\} \\
&= \frac{1}{4}e^{\left[-\frac{1}{2}\int^t\int^t\langle TO_1(\tau)O_1(\tau')\rangle+\langle TO_2(\tau)O_2(\tau')\rangle+\langle TO_1(\tau)O_2(\tau')\rangle+\langle TO_2(\tau)O_1(\tau')\rangle\right]}\left\{:e^{i(O_1+O_2)}:+:e^{-i(O_1+O_2)}:\right\} \\
&+\frac{1}{4}e^{\left[-\frac{1}{2}\int^t\int^t\langle TO_1(\tau)O_1(\tau')\rangle+\langle TO_2(\tau)O_2(\tau')\rangle-\langle TO_1(\tau)O_2(\tau')\rangle-\langle TO_2(\tau)O_1(\tau')\rangle\right]}\left\{:e^{i(O_1-O_2)}:+:e^{-i(O_1-O_2)}:\right\} \\
&\equiv \frac{1}{4}e^{-\frac{1}{2}T\mathcal{O}_+}\left\{:e^{i(O_1+O_2)}:+:e^{-i(O_1+O_2)}:\right\}+\frac{1}{4}e^{-\frac{1}{2}T\mathcal{O}_-}\left\{:e^{i(O_1-O_2)}:+:e^{-i(O_1-O_2)}:\right\}
\end{aligned}
$$

$$
T\mathcal{O}_+ \equiv \int^t\int^t\langle TO_1(\tau)O_1(\tau')\rangle+\langle TO_2(\tau)O_2(\tau')\rangle+\langle TO_1(\tau)O_2(\tau')\rangle+\langle TO_2(\tau)O_1(\tau')\rangle
$$

$$
T\mathcal{O}_- \equiv \int^t\int^t\langle TO_1(\tau)O_1(\tau')\rangle+\langle TO_2(\tau)O_2(\tau')\rangle-\langle TO_1(\tau)O_2(\tau')\rangle-\langle TO_2(\tau)O_1(\tau')\rangle
$$

$$
\begin{aligned}
&\langle U_0^\dagger(t) U_0(t)\rangle \\
&= \langle \left\{ \frac{1}{4} e^{-\frac{1}{2}\tilde{T}\mathcal{O}_+} \left[:e^{i(O_1+O_2)}: + :e^{-i(O_1+O_2)}: \right] + \frac{1}{4} e^{-\frac{1}{2}\tilde{T}\mathcal{O}_-} \left[:e^{i(O_1-O_2)}: + :e^{-i(O_1-O_2)}: \right] \right\} \\
&\left\{ \frac{1}{4} e^{-\frac{1}{2}T\mathcal{O}_+} \left[:e^{i(O_1+O_2)}: + :e^{-i(O_1+O_2)}: \right] + \frac{1}{4} e^{-\frac{1}{2}T\mathcal{O}_-} \left[:e^{i(O_1-O_2)}: + :e^{-i(O_1-O_2)}: \right] \right\} \rangle \\
&= \frac{1}{16} e^{-\frac{1}{2}\tilde{T}\mathcal{O}_+ - \frac{1}{2}T\mathcal{O}_+} \langle \left[:e^{i(O_1+O_2)}: + :e^{-i(O_1+O_2)}: \right] \left[:e^{i(O_1+O_2)}: + :e^{-i(O_1+O_2)}: \right] \rangle \\
&+ \frac{1}{16} e^{-\frac{1}{2}\tilde{T}\mathcal{O}_+ - \frac{1}{2}T\mathcal{O}_-} \langle \left[:e^{i(O_1+O_2)}: + :e^{-i(O_1+O_2)}: \right] \left[:e^{i(O_1-O_2)}: + :e^{-i(O_1-O_2)}: \right] \rangle \\
&+ \frac{1}{16} e^{-\frac{1}{2}\tilde{T}\mathcal{O}_- - \frac{1}{2}T\mathcal{O}_+} \langle \left[:e^{i(O_1-O_2)}: + :e^{-i(O_1-O_2)}: \right] \left[:e^{i(O_1+O_2)}: + :e^{-i(O_1+O_2)}: \right] \rangle \\
&+ \frac{1}{16} e^{-\frac{1}{2}\tilde{T}\mathcal{O}_- - \frac{1}{2}T\mathcal{O}_-} \langle \left[:e^{i(O_1-O_2)}: + :e^{-i(O_1-O_2)}: \right] \left[:e^{i(O_1-O_2)}: + :e^{-i(O_1-O_2)}: \right] \rangle \\
&= \frac{1}{16} e^{-\frac{1}{2}\tilde{T}\mathcal{O}_+ - \frac{1}{2}T\mathcal{O}_+} \left[2e^{-\frac{1}{2}\tilde{T}T\mathcal{O}_{++} - \frac{1}{2}T\tilde{T}\mathcal{O}_{++}} + 2e^{\frac{1}{2}\tilde{T}T\mathcal{O}_{++} + \frac{1}{2}T\tilde{T}\mathcal{O}_{++}} \right] \\
&+ \frac{1}{16} e^{-\frac{1}{2}\tilde{T}\mathcal{O}_+ - \frac{1}{2}T\mathcal{O}_-} \left[2e^{-\frac{1}{2}\tilde{T}T\mathcal{O}_{-+} - \frac{1}{2}T\tilde{T}\mathcal{O}_{-+}} + 2e^{\frac{1}{2}\tilde{T}T\mathcal{O}_{-+} + \frac{1}{2}T\tilde{T}\mathcal{O}_{-+}} \right] \\
&+ \frac{1}{16} e^{-\frac{1}{2}\tilde{T}\mathcal{O}_- - \frac{1}{2}T\mathcal{O}_+} \left[2e^{-\frac{1}{2}\tilde{T}T\mathcal{O}_{+-} - \frac{1}{2}T\tilde{T}\mathcal{O}_{+-}} + 2e^{\frac{1}{2}\tilde{T}T\mathcal{O}_{+-} + \frac{1}{2}T\tilde{T}\mathcal{O}_{+-}} \right] \\
&+ \frac{1}{16} e^{-\frac{1}{2}\tilde{T}\mathcal{O}_- - \frac{1}{2}T\mathcal{O}_-} \left[2e^{-\frac{1}{2}\tilde{T}T\mathcal{O}_{--} - \frac{1}{2}T\tilde{T}\mathcal{O}_{--}} + 2e^{\frac{1}{2}\tilde{T}T\mathcal{O}_{--} + \frac{1}{2}T\tilde{T}\mathcal{O}_{--}} \right]
\end{aligned}
$$

Still in progress …

$$
\begin{aligned}
\tilde{T}T\mathcal{O}_{++} &\equiv \int^t \int^t \langle \tilde{T}O_1 TO_1 \rangle + \langle \tilde{T}O_2 TO_2 \rangle + \langle \tilde{T}O_1 TO_2 \rangle + \langle \tilde{T}O_2 TO_1 \rangle \\
T\tilde{T}\mathcal{O}_{++} &\equiv \int^t \int^t \langle TO_1 \tilde{T}O_1 \rangle + \langle TO_2 \tilde{T}O_2 \rangle + \langle TO_2 \tilde{T}O_1 \rangle + \langle TO_1 \tilde{T}O_2 \rangle \\
\tilde{T}T\mathcal{O}_{--} &\equiv \int^t \int^t \langle \tilde{T}O_1 TO_1 \rangle + \langle \tilde{T}O_2 TO_2 \rangle - \langle \tilde{T}O_1 TO_2 \rangle - \langle \tilde{T}O_2 TO_1 \rangle \\
T\tilde{T}\mathcal{O}_{--} &\equiv \int^t \int^t \langle TO_1 \tilde{T}O_1 \rangle + \langle TO_2 \tilde{T}O_2 \rangle - \langle TO_2 \tilde{T}O_1 \rangle - \langle TO_1 \tilde{T}O_2 \rangle \\
\tilde{T}T\mathcal{O}_{+-} &\equiv \int^t \int^t \langle \tilde{T}O_1 TO_1 \rangle - \langle \tilde{T}O_2 TO_2 \rangle + \langle \tilde{T}O_1 TO_2 \rangle - \langle \tilde{T}O_2 TO_1 \rangle \\
T\tilde{T}\mathcal{O}_{+-} &\equiv \int^t \int^t \langle TO_1 \tilde{T}O_1 \rangle - \langle TO_2 \tilde{T}O_2 \rangle - \langle TO_2 \tilde{T}O_1 \rangle + \langle TO_1 \tilde{T}O_2 \rangle \\
\tilde{T}T\mathcal{O}_{-+} &\equiv \int^t \int^t \langle \tilde{T}O_1 TO_1 \rangle - \langle \tilde{T}O_2 TO_2 \rangle - \langle \tilde{T}O_1 TO_2 \rangle + \langle \tilde{T}O_2 TO_1 \rangle \\
T\tilde{T}\mathcal{O}_{-+} &\equiv \int^t \int^t \langle TO_1 \tilde{T}O_1 \rangle - \langle TO_2 \tilde{T}O_2 \rangle + \langle TO_2 \tilde{T}O_1 \rangle - \langle TO_1 \tilde{T}O_2 \rangle
\end{aligned}
$$

III. Robust Topological Qubits

Topological Qubits

- Consider a special case where the qubit is non-local, i.e., composed of 2 spatially separated Majorana modes. We call it topological qubit.

- We then couple this topological qubit to helical Luttinger liquid with Ohmic type spectral density.

- As two Majorana modes are far separated, then <O_1 O_2>=0. Thus, the previous 4-point correlator becomes product of two 2-point ones.

- This kind of topological qubits can be realized as the edge modes of the Kitaev's chain, 1d topological superconductor.

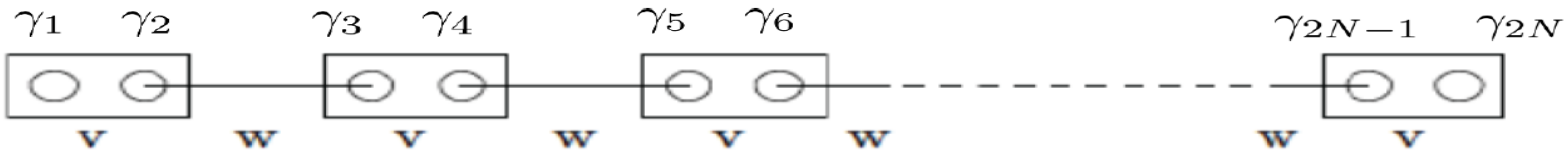

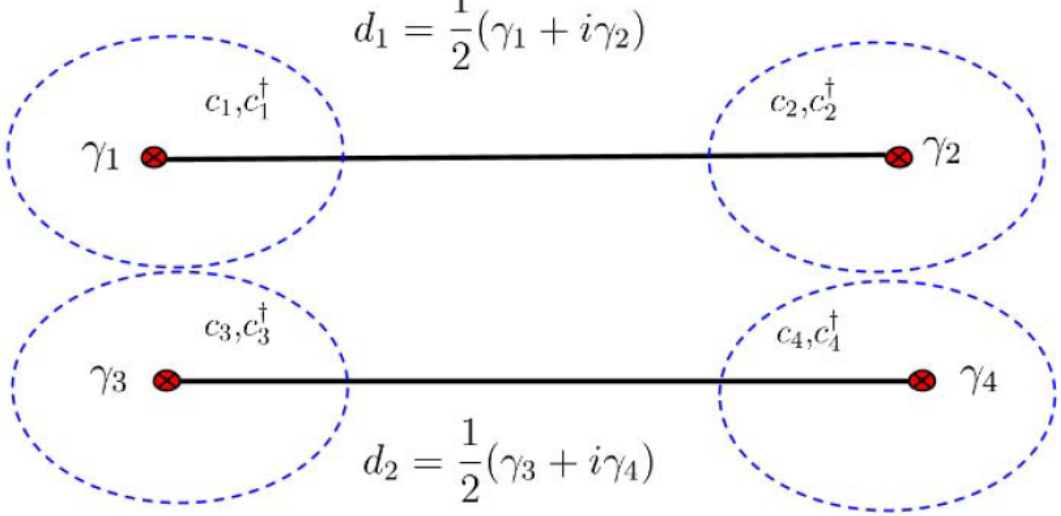

$$\sum_a B_a \gamma_a \mathcal{O}_a$$

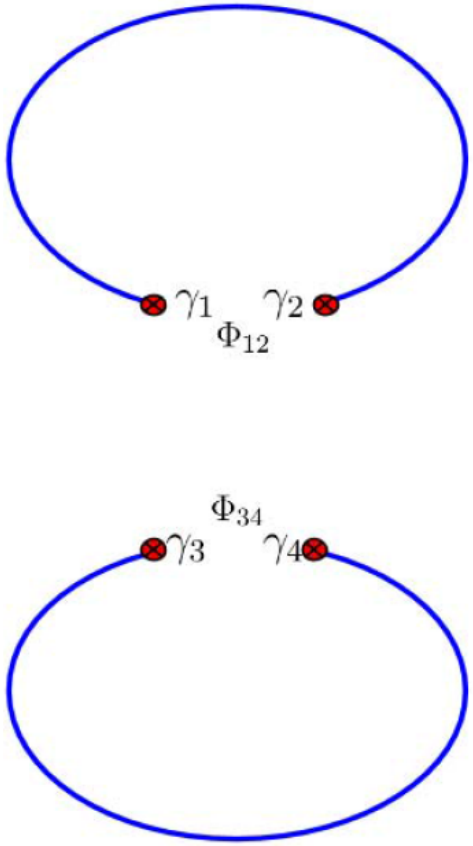

$$\sum_{a>b} B_{ab} \gamma_a \gamma_b \mathcal{O}_{ab}$$

Special features

- There is no retarded Green function appearing in the final form of the reduced dynamics. This implies that the Majorana modes/Helical liquid are dissipationless, i.e., generating no heat.

- The symmetric Green function appearing above is the Majorana-dressed one as discussed. It control the overall time dependence.

- Turn out that this time factor for Ohmic-like spectrum has a closed form, and has a critical point at Q=1.

Single topological qubit

1) Pure initial state: $\rho_{\mathcal{P}}(t=0) = \begin{pmatrix} a_{00} & a_{01} \\ a_{01} & a_{11} \end{pmatrix}$

$$\alpha(t) = e^{2B^2 \int^t d\tau \int^t d\tau' \overline{G}_{sym}(\tau-\tau')} = e^{-2B^2 |\alpha_{1,2}| I_Q(t;\mu=0,\Gamma_0)}$$

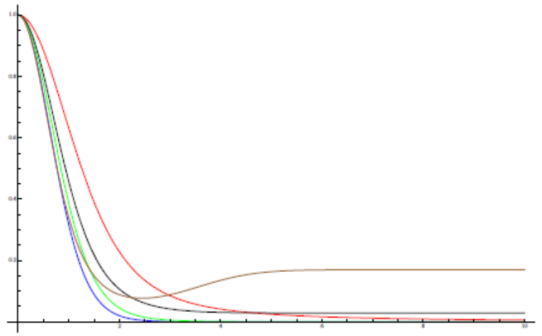

2) For Z2-preserving interactions:

$$\rho_r^b(t) = \begin{pmatrix} a_{00} & a_{01}\alpha(t) \\ a_{10}\alpha(t) & a_{11} \end{pmatrix}$$

3) For Z2-breaking interactions:

$$\rho_r^f(t) = \frac{1}{2}\begin{pmatrix} 1+(2a_{00}-1)\alpha^2(t) & 2a_{01}\alpha(t) \\ 2a_{10}\alpha(t) & 1+(2a_{11}-1)\alpha^2(t) \end{pmatrix}$$

4) The Z2 parity prevents from complete thermalization into Gibbs state.

Two Qubits: Special case for uniform environments

Before studying the reduced dynamics for more general initial states:

$$|(e_1, e_2, e_3, e_4)\rangle = e_1|00\rangle + e_2|01\rangle + e_3|10\rangle + e_4|11\rangle$$

with $|e_1|^2 + |e_2|^2 + |e_3|^2 + |e_4|^2 = 1$.

Let us first consider a simple case: choose the initial state as $|(e_1, 0, 0, e_4)\rangle$, i.e.,

$$\rho_{\mathcal{P}}(t=0) = \begin{pmatrix} |e_1|^2 & 0 & 0 & e_1 e_4^* \\ 0 & 0 & 0 & 0 \\ 0 & 0 & 0 & 0 \\ e_1^* e_4 & 0 & 0 & |e_4|^2 \end{pmatrix}$$

Fermionic:

$$\rho_r^f(t) = \frac{1}{4}\begin{pmatrix} A_{11} & 0 & 0 & A_{14} \\ 0 & A_{22} & 0 & 0 \\ 0 & 0 & A_{33} & 0 \\ A_{41} & 0 & 0 & A_{44} \end{pmatrix}$$

with $A_{11} = 1 + \alpha(t)^4 + 2(2|e_1|^2 - 1)\alpha(t)^2$, $A_{22} = A_{33} = 1 - \alpha(t)^2$,

$A_{44} = 1 + \alpha(t)^4 + 2(2|e_4|^2 - 1)\alpha(t)^2$ and $A_{14} = A_{41}^* = 4e_1 e_4^* \alpha(t)^2$

Bosonic:

$$\rho_r^b(t) = \begin{pmatrix} |e_1|^2 & 0 & 0 & e_1 e_4^* \alpha(t)^2 \\ 0 & 0 & 0 & 0 \\ 0 & 0 & 0 & 0 \\ e_1^* e_4 \alpha(t)^2 & 0 & 0 & |e_4|^2 \end{pmatrix}$$

Two T-qubits in fermonic environments

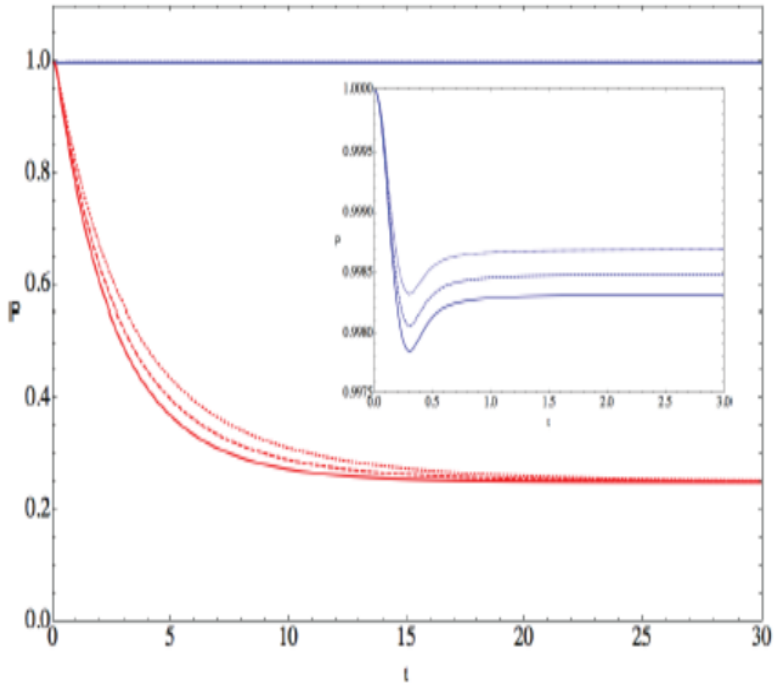

FIG. 4: Purity vs t for $\kappa = 0.5$ (red) and $\kappa = 2$ (blue) with initial states $|(e_1, e_2, e_3, e_4)\rangle = |(1, 0, 0, 1)\rangle$ (solid), $|(2, 1, 0, 2)\rangle$ (dashed), $|(1, 1, 0, 1)\rangle$ (dotted). The inset is to magnify the early time region of $\kappa = 2$ cases.

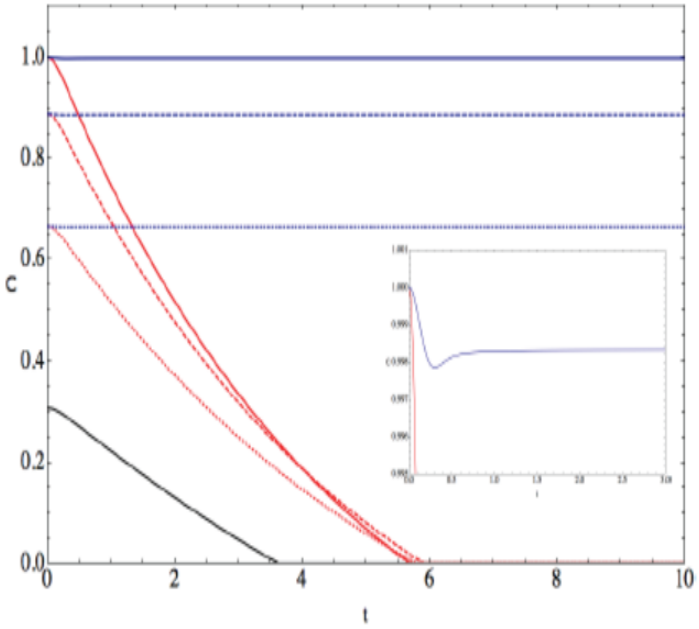

FIG. 5: Concurrence vs t for the states and environments specified in Fig. 4. The inset shows the solid lines enlarged at short time. Here we add a black solid line representing the concurrence pattern of the initial state $|(e_1, e_2, e_3, e_4)\rangle = |(2, 2, 1, 2)\rangle$ in the $\kappa = 0.5$ environment to show its concurrence does not diminish with the other red lines at the same time.

C.f. Spin-Boson model

ref. S.T. Wu PRA89p034301, also H.B. Liu et al, PRA87p052139

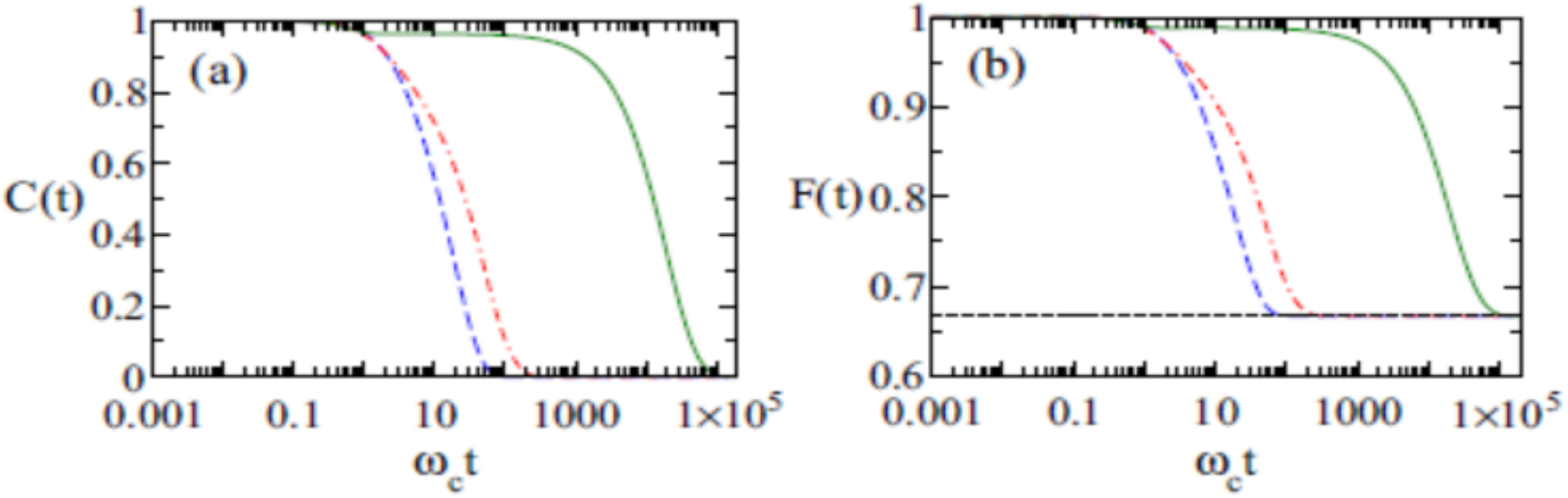

FIG. 3. (Color online) Time evolution for the (a) concurrence and (b) maximum teleportation fidelity for the Bell state (12) at weak environment coupling ($\eta_0 = 0.01$) when the spectral function is sub-Ohmic ($s = 1/2$, blue dashed curves), Ohmic ($s = 1$, red dot-dashed curves), and super-Ohmic ($s = 3$, green solid curves). The horizontal dashed line in (b) indicates the classical limit $F = \frac{2}{3}$.

Effective gap-ness

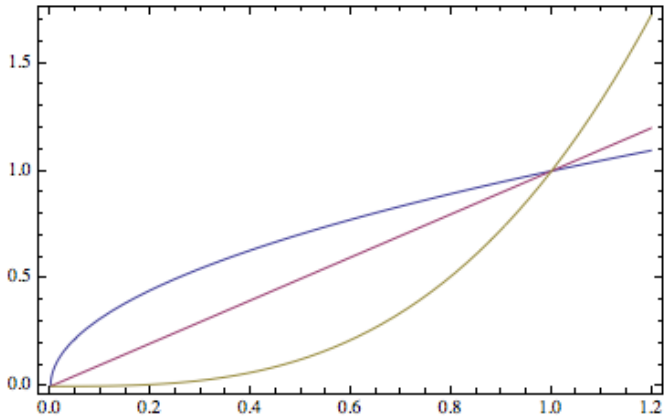

- The quantum information of the probe is carried away by the collective excitations of the environment, which is specified by the spectral density.
- The Ohmic-like spectrum has no gap at low energy, and one would expect the complete decoherence.
- However, the super-Ohmic spectrum suppress more the low energy modes than the higher energy ones.
- Adding the topological nature of the Majorana modes, we see an effective gap emerging for super-Ohmic cases.

Non-uniform environments

- As the topological qubit is non-local, one can then couple its component Majorana modes to different environments. This is peculiar feature of the topological qubits.

- One can couple one of the Majorana modes to the sub-Ohmic environment and another one to the super-Ohmic one. Then, the decoherence pattern will depend on the initial states.

- Some peculiar patterns for the decoherece and concurrence can be obtained in such cases.

Summary

- The deocherence in holographic CFT environment is similar to the helical Luttinger ones. It is interesting to consider other holographic environments.

- The trick of decomposing spinless fermion into 2 Majorana modes yields the closed form of RDM.

- Robust topological qubits are viable at least theoretically.